Automatic Motion Artifact Removal in ECG with Canonical Polyadic Decomposition

Jannis Lilienthal and Waltenegus Dargie
Technische Universität Dresden
01062 Dresden, Germany
{jannis.lilienthal, waltenegus.dargie}@tu-dresden.de

***Abstract*—The electrocardiogram (ECG) is a reliable tool for monitoring cardiac conditions non-invasively. Its use is nowadays widespread and extends beyond purely medical purposes. Nevertheless, its application in residential settings comes with drawbacks. Non-stationary noise caused by motion reduces the signal's quality and alters the signal's characteristics. In this paper, we employ canonical polyadic decomposition (CPD) along with the measurements of a 3D accelerometer to characterize and remove artifacts. A CPD decomposes a noisy ECG into its constituting elements by examining multi-dimensional correlations. Its success, however, depends on how well the constituting elements are estimated to configure the model. The purpose of this paper is to achieve this task. We recorded data from ten healthy subjects undertaking different movement types: *Standing up*, *bending forward*, *walking*, *running*, *jumping*, and *climbing stairs*. In addition, we recorded isolated motion artifacts from the back of the subjects and mixed them with the ECG signals. To quantify the performance of the decomposition process, we compared the difference in the signal-to-noise ratio (SNR) and the root mean squared error (RMSE) between the actual and the estimated ECG. The proposed CPD model outperforms the adaptive filter and the wavelet denoising in terms of the SNR.**

***Index Terms*—inertial sensor, motion artifact, tensor decomposition, unsupervised machine learning, wireless electrocardiogram**

I. Introduction

Cardiovascular diseases (CVDs) remain the leading cause of death with a share of 31 % in all global deaths [1]. Early detection is vital to start the appropriate treatment at early onset and minimize the risk of a fatal outcome. Therefore, the electrocardiogram (ECG) is the most commonly applied method. Its application is straightforward, non-invasive, and the information derived is highly diagnostic. Recently, many mobile monitoring devices have been developed that include, among others, ECG sensors to record cardiovascular. By employing these devices in residential settings, they reduce the need for constant supervision by medical experts and decrease healthcare costs. [2], [3] The continuous technical development has led to increased comfort and more comfortable use in everyday life.

However, the added freedom of movement has also led to many limitations and drawbacks. The subjects' movement causes significant artifacts, which hinder the automated evaluation of the data. These motion artifacts can mimic severe pathological conditions of the heart [4], and they can lead to significant misinterpretation of underlying conditions [5]. Therefore, they need to be removed from the data before it is evaluated.

Unfortunately, motion artifacts and cardiac information in the ECG inherit significant overlap in their spectral characteristics [6]. Therefore, traditional linear frequency filtering fails to separate them. Previously, various methods have been proposed to remove motion artifacts from the ECG: The adaptive filter (AF) uses a reference signal (e.g., an accelerometer) that is correlated to the motion artifacts to estimate the noise present in the ECG [7], [8]. Independent component analysis (ICA) is a matrix decomposition method that factorizes multi-channel ECG based on the assumption that artifacts and cardiac information are statistically independent [9]. Wavelet transform (WT) transforms the ECG from the time into the time-frequency space and eliminates motion artifacts by a) removing cardiac information and considering the residuals as artifacts [10] or b) removing the motion artifacts by employing multi-level thresholding with thresholds specifically modified to remove motion artifacts directly [11].

In the following, we propose a method based on tensor decomposition to remove motion artifacts. Furthermore, we demonstrate how to estimate the required tensor rank using statistical parameters and remove the artifacts using an accelerometer as a motion reference. This paper extends a previous publication [12], in which we demonstrated the ability of tensor decomposition to remove motion artifacts from ECG with for a selected signal-to-noise ratio (SNR) using a fixed decomposition rank. Accordingly, in the following, we present an approach that can predict the rank of the decomposition and show that the removal of artifacts with tensor is applicable to different noise levels.

We organize the paper as follows: In section II, we give a brief introduction to tensor decomposition. In section III, we describe our approach to remove artifacts, including the experimental setup, and discuss the results in section IV.

II. Tensor Decomposition

Matrix factorization belongs to the family of unsupervised machine learning algorithms. This technique is employed to extract underlying information from data by decomposing a matrix into latent factors. Figure 1 illustrates the principle of matrix factorization for the singular value decomposition (SVD). The matrix $\mathbf{X}$ is decomposed into an outer product of the left

This work has been funded by the German Research Foundation (DFG) under the project agreements DA 1211/7-1 (RoReyBaN).

and right singular vectors $\mathbf{u}_r$ and $\mathbf{v}_r$, scaled by the respective singular value σ_r. SVD factorizes a matrix into R components by assuming that these components are orthogonal to each other. In order to remove motion artifacts, artifacts and cardiac information would thus have to be orthogonal. Similarly to SVD, other matrix decompositions impose different constraints, e.g., independence or non-negativity, to factorize the data.

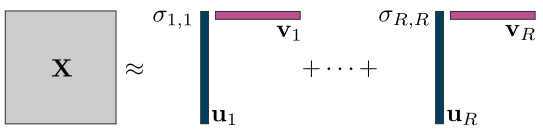

Figure 1. The principle of SVD [12].

Therefore, matrix decompositions heavily rely on enforcing artificial constraints on the factors (independence, orthogonality). Furthermore, the number of components that can be extracted is limited to the number of input channels used in the decomposition process (i.e., a two-channel ECG yields no more than two components extracted).

In contrast to matrix decomposition, tensor decomposition is applied to N-dimensional data, where $N \geq 3$. It utilizes the multi-dimensional correlation existing in the data to extract latent information instead of imposing additional constraints. In contrast to matrix decomposition, the number of sources extracted is not limited by the original data.

One of the most frequently employed tensor decomposition models is canonical polyadic decomposition (CPD). CPD is a rank-based factorization method that decomposes a tensor $\mathcal{X}$ into a linear combination of rank-one tensors (also referred to as pure tensor). For a three-dimensional tensor, the CPD model is defined as:

$$\mathcal{X} \approx \sum_{r=1}^{R} \mathbf{a}_r \circ \mathbf{b}_r \circ \mathbf{c}_r \tag{1}$$

where $\circ$ is the outer product, R is the rank of the model, quantifying the latent features extracted, and $\mathbf{a}_i, \mathbf{b}_i, \mathbf{c}_i$ are the three loading vectors, each representing one dimension of the initial tensor $\mathcal{X}$. Figure 2 illustrates this model for the three-dimensional case.

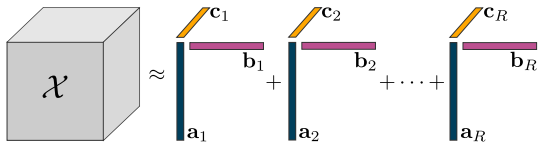

Figure 2. The principle of CPD for a three-dimensional tensor [12].

One of the shortcomings of CPD is the need for a priori information on the decomposition rank R. In matrix factorization, this can, however, be done automatically. In the following, we will therefore introduce an approach to automatically remove motion artifacts from the ECG by predicting the tensor rank based on readily available statistical signal characteristics.

III. Algorithm

Our approach's basic premise is combining the measurements from a reference sensor (e.g., accelerometer) and the noisy ECG. Because the reference sensor picks up the body movements, it inevitably characterizes the motion artifacts. By combining the data from the accelerometer and the ECG, we apply CPD to extract features that the two sensor types have in common – these will yield the motion artifacts. The extracted artifacts can subsequently be subtracted from the noisy ECG. Figure 3 depicts the process for artifact removal that we employed and which will be explained more precisely in the following.

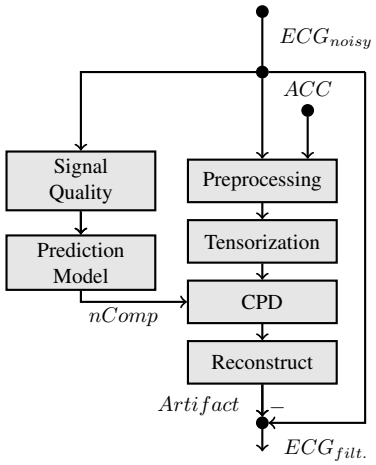

Figure 3. Framework for artifact removal using CPD.

A. Experimental Setup and Data Acquisition

We employed the *Shimmer3* platform [13] to measure the cardiac activity and characterize the movements performed using the reference sensor. The *Shimmer3* platform integrates, among others, an ECG and an accelerometer. We recorded 120 s data at 512 Hz from ten healthy subjects in rest and while performing various physical activities. Our selection of movements was based on the diverse aspects of everyday life and accommodates high impact movements (running, jumping, and climbing stairs) and movements of moderate-intensity (standing up, bending forward, and walking). We tried to make the executions of the movements as natural as possible. Only bending forward, standing up, and jumping were stationary, meaning they were performed on the spot.

B. Preprocessing and Tensorization

We preprocessed all data by employing a bandpass filter between 0.5–150 Hz to remove noise outside of the spectral range containing valuable cardiac information. The selection of cutoff frequencies was based on a recommendation by the American Heart Association (AHA) [14]. They recommend employing a low-frequency cutoff of 0.05 Hz for routine filters, which can be relaxed to 0.5 Hz for linear digital filters with zero phase distortion.

Typically, ECG measurements are available as a vector (single-channel) or matrix (multi-channel). Therefore, the

ECG needs to be transformed into a tensor before applying CPD – this process is called *tensorization*. A commonly applied method is employing time-frequency transformations to transform signals into the time-frequency space. One possibility for this are so-called wavelet transformations. These methods use a base function that is scaled and shifted through the signal to capture low and high frequency components in the data. Thereby, wavelet transformations maintain a high frequency resolution for low frequencies and a high time resolution for high frequencies, making its application suitable to capture the broad range of spectral characteristics in the ECG.

We apply the maximal overlap discrete wavelet transform (MODWT) with the *Haar* wavelet as mother wavelet to transform the ECG and the accelerometer into the time-frequency space. The MODWT is a variant of the discrete wavelet transform (DWT) that is translation-invariant, i.e., the signal is invariant against shifts in the time domain. In contrast to DWT, the temporal features of the data (i.e., R peak) remain aligned and are not shifted with each wavelet level.

Both sensor data are now made up by the dimensions *samples* $\times$ *scale*. *Note:* The dimension *scale* results from the scaled versions of the base function of the MODWT. It is inversely proportional to the frequency. In our case, each matrix contains 13 different wavelet scales providing access to the signals' temporal and spectral features. Figure 4 illustrates how the wavelet transformed ECG and accelerometer (in matrix shape) are combined to form a three-dimensional tensor. The tensor is then made up by the dimensions: *channel* $\times$ *samples* $\times$ *scale*. With that, the CPD can explore temporal, spectral, and spatial (across channels) correlations in the data to find latent features.

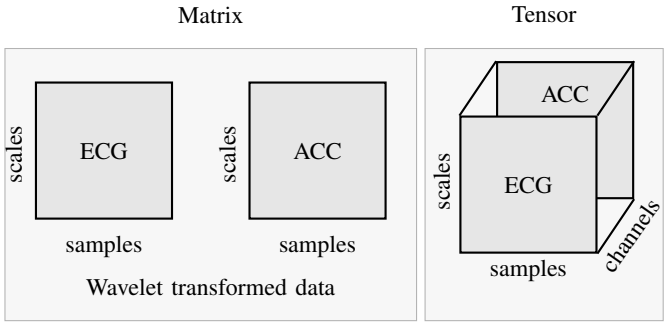

Figure 4. Tensorization: Constructing a tensor from two matrices.

C. Evaluation

One of the key aspects of motion artifact removal is objectively evaluating the approach. The ECG can either be recorded from a subject in motion, resulting in noise corrupting the signal, or in rest, providing a noise-free ECG. However, due to the non-stationary characteristics of ECG signals, the noise-free segments cannot be used to evaluate artifact removal in the noisy segments. This means that the heart naturally beats irregularly, and one heartbeat is not identical to the next. As a result, a segment recorded at rest cannot be used to evaluate artifact removal in subsequent motion segments because the underlying cardiac information has changed and is unknown.

Artificially corrupted data are regularly employed to assess the performance of motion artifact removal methods [7], [15]. Therefore, isolated artifacts need to be available to combine them with clean ECG segments.

We placed one sensor node at the back of each subject around the height of the lumbar curve, where cardiac influence is assumed to be negligible [7], [15], to record a single-channel ECG and the acceleration. Because the cardiac information delivered is marginal, motion artifacts dominate the ECG recorded there. These artifacts can subsequently be added to a clean ECG taken from the front of the torso in rest to generate artificially corrupted signals. Figure 5 illustrates the arrangement of the electrodes and the sensor nodes at the front and the back.

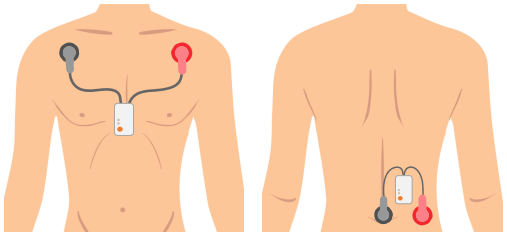

(a) Front (b) Back

Figure 5. Sensor node and electrode placement to record ECG and isolated motion artifacts.

Subsequently, we can generate artificially corrupted ECG s_{art} by combing the clean ECG $s_{cardiac}$ with the isolated motion artifact a_{motion}:

$$s_{art}(t) = s_{cardiac}(t) + a_{motion}(t) \tag{2}$$

We recorded the ECG in rest and motion from a total of ten subjects. Thus, for each movement type, there exist ten recordings of isolated motion artifacts. We subsequently used these artifacts and added them to the clean ECG from all ten subjects. Therefore, for each movement, 100 noisy ECG with the respective noise-free ECG are available. The following metrics can then be employed to quantify the artifact removal method:

$$\mathrm{RMSE} = \sqrt{\frac{1}{n}\sum_{i=1}^{n}(s_i - \hat{s}_i)^2} \tag{3}$$

$$\mathrm{SNR}_{dB} = 10\log_{10}\left(\frac{P_{\mathrm{signal}}}{P_{\mathrm{noise}}}\right) \tag{4}$$

where the root mean squared error (RMSE) quantifies the error between the clean ECG s and its estimation $\hat{s}$ and the SNR quantifies the power of the signal P_{signal} with respect to the power of the noise P_{noise}.

D. Rank Estimation

The central parameter for the CPD model is the decomposition rank, which must be defined before the data can be

decomposed. A commonly applied method to estimate the tensor rank is core consistency diagnostic (CONCORDIA). CONCORDIA requires the iterative computation of the CPD model for a large number of different decomposition ranks. Subsequently, the best rank can be determined based on the core consistency of each computed model. However, this method is computationally intense because the number of iterations until convergence varies, and the repeated computation of the CPD model is time-consuming. Alternative methods for rank estimation (RELFIT, LOSS function) similarly apply iterative techniques, which are impractical for mobile ECG due to the time and resource requirements. [16]

In the following, we propose a method to avoid iterative operations by considering statistical parameters of the noisy ECG. Therefore, we investigated the relationship between the model rank and the performance in motion artifact removal concerning the SNR. We employed CPD models with varying rank of $n_{rank} \in [1, 15]$ to remove motion artifacts from the ECG with a fixed rank (refer to Fig. 3). The upper limit was chosen as our analysis indicated that higher ranks yielded strongly correlated components, a phenomenon also described in [17]. We generated artificially corrupted ECG with SNR in the range of −10 dB to 5 dB to simulate different corruption levels. The goal is to **1)** identify the rank that yields the highest SNR and **2)** find a parameter that can be used to predict this rank.

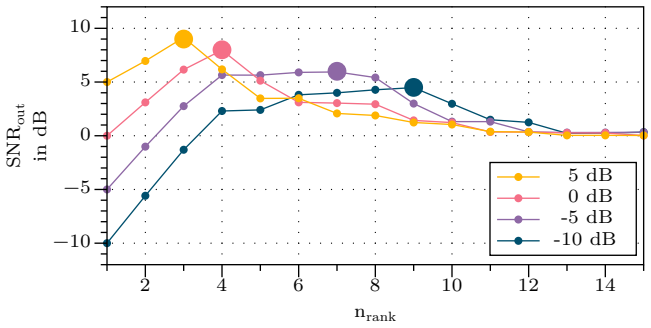

Figure 6. SNR as a function of the decomposition rank.

Figure 6 depicts the SNR after motion artifact removal with a CPD model for bending forward at four noise levels. It is apparent that the optimal decomposition rank depends on the SNR level in the noisy ECG. For all movements, the rank is strongly correlated to the SNR in the signal ($R_{corr} = -0.82$), i.e., a higher rank is required if the noise in the signal is stronger. Unfortunately, the SNR can not be determined in advance because detailed knowledge of the noise contaminating the signal is required.

Thus we considered commonly employed statistical parameters that characterize the ECG quality and quantify the noise level. These signal quality indices (SQIs) are readily accessible and can be computed without the knowledge of the signals' actual noise (refer to [18]) at low computational costs. The following parameters were applied to estimate the model rank:

kSQI Kurtosis: The noise-free ECG is expected to be highly non-Gaussian since it is not random. [18], [19]

sSQI Skewness: The noise-free ECG is expected to be highly skewed due to the QRS complex. [18]–[20]

iorSQI Ratio between the signal power inside the QRS complex band (5–40 Hz) and outside of this band. [19]

pSQI Relative power in the narrowed QRS complex band (5–15 Hz). [18], [21]

basSQI Relative power in the baseline band 0–1 Hz with respect to the power in the interval 0–40 Hz. [18], [19], [21]

A linear regression algorithm was employed to predict the model rank based on these SQI. Therefore, the regression model was trained using the best decomposition rank n_{best} as response variable y and the five SQIs as the predictors $x_{1...5}$.

Our approach was subsequently validated by employing cross-validation (CV) to avoid the already known best rank for a particular subject and movement to influence the prediction model. We excluded each subject once from training data and trained the linear model with the remaining data (best rank and SQIs). This model was subsequently employed to predict the rank and remove the motion artifacts according to Figure 3.

IV. Results

To quantify the results, we considered the SNR before artifact removal and afterward. Similarly, we calculated the RMSE between the noisy ECG respectively the denoised ECG and the clean ECG. Table I illustrates the results of our proposed method as the mean value over the six movement types considered.

We compared the approach to two methods that are established in the literature. The AF uses the accelerometer as a reference for the motion artifacts and was implemented using least mean square (LMS) optimization [8]. Secondly, we employed a method that is based on wavelet denoising, which modifies specific wavelet coefficients to remove the artifacts [10].

Table I
Comparison of the performance in motion artifact removal with reference methods.

Method	**SNR** in dB		**RMSE**	
	before	after	before	after
CPD	-10	0.3	0.15	0.11
	-5	0.8	0.13	0.10
	0	2.0	0.10	0.09
	5	4.4	0.06	0.07
LMS-AF	-10	-4.5	0.15	0.21
	-5	-1.4	0.13	0.15
	0	-0.5	0.10	0.11
	5	-1.6	0.06	0.10
Wavelet Denoising	-10	-6.0	0.15	0.25
	-5	-1.9	0.13	0.16
	0	1.1	0.10	0.11
	5	2.9	0.06	0.09

The CPD model outperforms the LMS-AF and the wavelet denoising method in both SNR and RMSE. The SNR can be increased up to $\Delta\,\mathrm{SNR} = 10.3\,\mathrm{dB}$.

Furthermore, the enhanced performance of the CPD model is also reflected in visual artifact removal. Figure 7 illustrates the results for one subject performing the movement bending forward. *Note:* The varying R peak amplitude for CPD results from scaling operations and is not related to the artifact removal method itself. It is apparent that CPD removes the motion artifacts more reliably. While the LMS-AF removes artifacts, it also removes P waves and introduces additional signal alterations at the beginning of the segment. The wavelet denoising approach removes the majority of the high frequency noise by smoothing the signal. However, the signal characteristics are also modified (e.g., R peak). This is likely because the method is primarily based on detecting outliers and modifying their wavelet coefficients. However, movements in everyday life are instead executed continuously for a certain time, which produces persistent interferences.

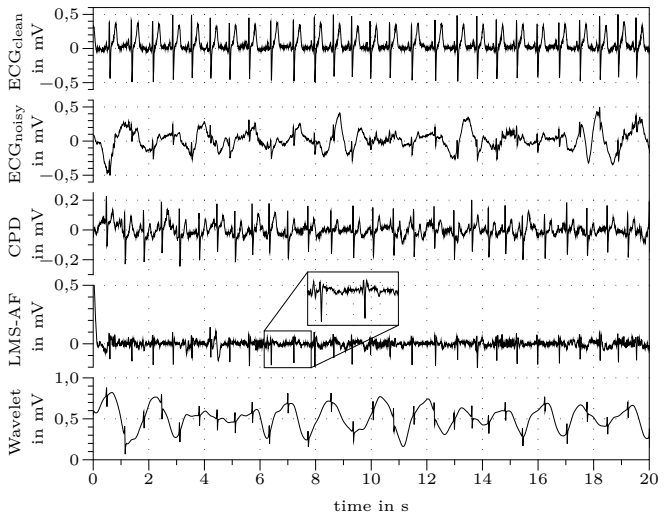

Figure 7. Comparison of motion artifact removal with state of the art for an SNR of −10 dB.

V. Conclusion

This paper employed canonical polyadic decomposition combining the measurements from ECG and an accelerometer to remove motion artifacts. Thereby, we extracted mutual features – the motion artifacts – and removed them from the noisy ECG. We proposed a method to predict the decomposition rank based on readily accessible statistical signal quality parameters. The approach was evaluated by artificially corrupting clean ECG segments with genuine motion artifacts generated at isolated locations. The results suggest that CPD can successfully remove motion artifacts for various movement types and outperforms two commonly employed artifact removal methods.

In the future, we intend to intensify our research on tensor decomposition. Advanced decomposition strategies that allow more flexible interactions between the factors, e.g., block term decomposition, might improve artifact removal.

References

[1] World Health Organization, "Global Health Estimates 2016: Deaths by Cause, Age, Sex, by Country and by Region, 2000-2016. Geneva: WHO, 2018," World Health Organization, Geneva, Tech. Rep., 2019.

[2] J. H. E. Yong, K. Thavorn, J. S. Hoch, *et al.*, "Potential Cost-Effectiveness of Ambulatory Cardiac Rhythm Monitoring after Cryptogenic Stroke," *Stroke*, vol. 47, no. 9, pp. 2380–2385, 2016.

[3] R. Jansi, R. Amutha, and S. Radha, "Remote monitoring of children with chronic illness using wearable vest," *Telemedicine Technologies: Big Data, Deep Learning, Robotics, Mobile and Remote Applications for Global Healthcare*, pp. 121–137, 2019.

[4] M. F. Márquez, L. Colín, M. Guevara, *et al.*, "Common electrocardiographic artifacts mimicking arrhythmias in ambulatory monitoring," *American Heart Journal*, vol. 144, no. 2, pp. 187–197, 2002.

[5] N. El-Sherif and G. Turitto, "Ambulatory electrocardiographic monitoring between artifacts and misinterpretation, management errors of commission and errors of omission," *Annals of Noninvasive Electrocardiology*, vol. 20, no. 3, pp. 282–289, 2015.

[6] N. V. Thakor, J. G. Webster, and W. J. Tompkins, "Estimation of QRS Complex Power Spectra for Design of a QRS Filter," *IEEE Transactions on Biomedical Engineering*, vol. BME-31, no. 11, pp. 702–706, Nov. 1984.

[7] I. Romero, D. Geng, and T. Berset, "Adaptive filtering in ECG denoising: A comparative study," *Computing in Cardiology*, vol. 39, pp. 45–48, 2012.

[8] S.-H. Liu, "Motion Artifact Reduction in Electrocardiogram Using Adaptive Filter," *Journal of Medical and Biological Engineering*, vol. 31, no. 1, p. 67, Aug. 2011.

[9] M. Milanesi, N. Martini, N. Vanello, *et al.*, "Independent component analysis applied to the removal of motion artifacts from electrocardiographic signals," *Medical & Biological Engineering & Computing*, vol. 46, no. 3, pp. 251–261, Mar. 2008.

[10] F. Strasser, M. Muma, and A. M. Zoubir, "Motion artifact removal in ECG signals using multi-resolution thresholding," *European Signal Processing Conference*, no. Eusipco, pp. 899–903, 2012.

[11] M. Kirst, B. Glauner, and J. Ottenbacher, "Using DWT for ECG motion artifact reduction with noise-correlating signals," in *Annual International Conference of the IEEE Engineering in Medicine and Biology Society*, IEEE, Aug. 2011, pp. 4804–4807.

[12] J. Lilienthal and W. Dargie, "Application of Tensor Decomposition in Removing Motion Artifacts from the Measurements of a Wireless Electrocardiogram," in *2020 IEEE 23rd International Conference on Information Fusion (FUSION)*, IEEE, Jul. 2020, pp. 1–8.

[13] A. Burns, B. R. Greene, M. J. McGrath, *et al.*, "SHIMMER - A wireless sensor platform for noninvasive biomedical research," *IEEE Sensors Journal*, vol. 10, no. 9, pp. 1527–1534, Sep. 2010.

[14] P. Kligfield, L. S. Gettes, J. J. Bailey, *et al.*, "Recommendations for the Standardization and Interpretation of the Electrocardiogram," *Circulation*, vol. 115, no. 10, pp. 1306–1324, Mar. 2007.

[15] D. Buxi, S. Kim, N. Van Helleputte, *et al.*, "Correlation between electrode-tissue impedance and motion artifact in biopotential recordings," *IEEE Sensors Journal*, vol. 12, no. 12, pp. 3373–3383, 2012.

[16] R. Bro and H. A. Kiers, "A new efficient method for determining the number of components in PARAFAC models," *Journal of Chemometrics*, vol. 17, no. 5, pp. 274–286, 2003.

[17] R. Bro, "PARAFAC. Tutorial and applications," *Chemometrics and Intelligent Laboratory Systems*, vol. 38, no. 2, pp. 149–171, 1997.

[18] U. Satija, B. Ramkumar, and M. Sabarimalai Manikandan, "A Review of Signal Processing Techniques for Electrocardiogram Signal Quality Assessment," *IEEE Reviews in Biomedical Engineering*, vol. 11, pp. 36–52, 2018.

[19] M. Nardelli, A. Lanata, G. Valenza, *et al.*, "A tool for the real-time evaluation of ECG signal quality and activity: Application to submaximal treadmill test in horses," *Biomedical Signal Processing and Control*, vol. 56, p. 101 666, 2020.

[20] J. Behar, J. Oster, Q. Li, *et al.*, "ECG signal quality during arrhythmia and its application to false alarm reduction," *IEEE Transactions on Biomedical Engineering*, vol. 60, no. 6, pp. 1660–1666, 2013.

[21] Z. Zhao and Y. Zhang, "SQI quality evaluation mechanism of single-lead ECG signal based on simple heuristic fusion and fuzzy comprehensive evaluation," *Frontiers in Physiology*, vol. 9, no. JUN, pp. 1–13, 2018.